

Probing neutron-skin thickness with free spectator neutrons in ultracentral high-energy isobaric collisions

Lu-Meng Liu,¹ Chun-Jian Zhang,² Jia Zhou,^{3,1} Jun Xu,^{4,3,*} Jiangyong Jia,^{2,5,†} and Guang-Xiong Peng^{6,7,8}

¹*School of Physical Sciences, University of Chinese Academy of Sciences, Beijing 100049, China*

²*Department of Chemistry, Stony Brook University, Stony Brook, NY 11794, USA*

³*Shanghai Institute of Applied Physics, Chinese Academy of Sciences, Shanghai 201800, China*

⁴*Shanghai Advanced Research Institute, Chinese Academy of Sciences, Shanghai 201210, China*

⁵*Physics Department, Brookhaven National Laboratory, Upton, NY 11976, USA*

⁶*School of Nuclear Science and Technology, University of Chinese Academy of Sciences, Beijing 100049, China*

⁷*Theoretical Physics Center for Science Facilities,*

Institute of High Energy Physics, Beijing 100049, China

⁸*Synergetic Innovation Center for Quantum Effects & Applications,*

Hunan Normal University, Changsha 410081, China

(Dated: March 21, 2022)

We propose that the yield ratio of free spectator neutrons produced in ultracentral relativistic $^{96}\text{Zr}+^{96}\text{Zr}$ to $^{96}\text{Ru}+^{96}\text{Ru}$ collisions is a robust probe of the neutron-skin thickness Δr_{np} of colliding nuclei and the slope parameter L of symmetry energy. The idea is demonstrated based on the proton and neutron density distributions of ^{96}Zr and ^{96}Ru from the Skyrme-Hartree-Fock model, and a Glauber model that provides information of spectator matter, where free neutrons are produced from the deexcitation of heavy clusters through the GEMINI model and direct ones that have not coalesced into light clusters through a Wigner function approach. A larger Δr_{np} associated with a larger L value increases the isospin asymmetry of spectator matter and thus leads to more free neutrons, especially in ultracentral collisions where the multiplicity of free neutrons are not affected by uncertainties of cluster formation and deexcitation. The ratio of neutron multiplicities in isobaric collision systems reduces the theoretical and experimental uncertainties, and is insensitive to the nuclear deformation effects.

Introduction. The distributions of protons and neutrons in heavy nuclei are the primary probes of the nuclear interaction as well as the nuclear matter equation of state (EOS) [1, 2], particularly the symmetry energy that describes how the energy per nucleon changes with the neutron-proton asymmetry [3]. In heavy neutron-rich nuclei, the excess neutrons are pushed out to form a neutron skin, with its thickness Δr_{np} defined as the difference between the neutron and proton root-mean-square (RMS) radii. The value of Δr_{np} is a robust probe of the slope parameter L of symmetry energy [4–9]. Besides its relevance in nuclear structure, the measurement of Δr_{np} and the subsequent determination of L are important in understanding many interesting phenomena in both astrophysics [10, 11] and nuclear reactions [12].

In the past decades, various methods have been used to measure Δr_{np} , including hadron-nucleus scatterings [13–18], photon-nucleus scatterings [19], and, particularly, parity-violating electron-nucleus scatterings [20, 21], the data from which has recently induced considerable attention [22] and debate [23, 24]. Recently, it is realized that the huge amount of particles produced in high-energy heavy-ion collisions at $\sqrt{s_{\text{NN}}} \gtrsim 100$ GeV can be used to determine the collective structure of colliding nuclei [25–27], including its neutron skin [28]. These collisions produce a hot dense matter known as the quark-

gluon plasma (QGP), whose space-time evolution is well described by relativistic hydrodynamics. The latter in turn can be used to image the shape and radial structures of the colliding nuclei [29]. The best example for this possibility is illustrated by comparing $^{96}\text{Ru}+^{96}\text{Ru}$ and $^{96}\text{Zr}+^{96}\text{Zr}$ collisions at $\sqrt{s_{\text{NN}}} = 200$ GeV. The ratios of many observables between these two isobaric systems, published by the STAR Collaboration [30], show significant deviations from unity, each with its own characteristic centrality dependencies. Since isobar nuclei have the same mass number, these deviations must originate from the difference in the structure of the colliding nuclei, which impact the initial state of QGP and its final state observables. Model calculations show that the ratios of elliptic flow v_2 and triangular flow v_3 suggest a large quadrupole deformation β_2 in ^{96}Ru and a large octupole deformation β_3 in ^{96}Zr , respectively [31]. In mid-central collisions, the ratio of v_2 and multiplicity distribution are consistent with a larger Δr_{np} in ^{96}Zr than in ^{96}Ru [28, 32]. Predictions for many other observables and their sensitivities to the deformation and neutron skin have been made, such as the mean transverse momentum p_{T} [33] and its fluctuations [34], and v_n - p_{T} correlations [27, 35, 36].

Most observables in heavy-ion collisions utilize particles produced near the mid-rapidity region, the description of which requires sophisticated modeling of the full space-time dynamics and properties of the QGP. In this paper, we propose the ratio of the number of free spectator neutrons N_n in isobar systems, easily measurable by

* Correspond to xujun@zjlab.org.cn

† Correspond to jiangyong.jia@stonybrook.edu

the zero-degree calorimeters (ZDC), as a clean and complementary probe of the neutron-skin thicknesses of ^{96}Zr and ^{96}Ru . In ultracentral collisions (UCC), most free spectator nucleons, outside the overlap region, originate from the surface of the nucleus (see cartoon in Fig. 1). Thanks to the extremely high speed of colliding nuclei in relativistic heavy-ion collisions, these free neutrons do not have a chance to interact with the matter produced by the participating nucleons and are captured by the ZDC. The N_n is sensitive to the Δr_{np} , i.e., a larger Δr_{np} in ^{96}Zr than in ^{96}Ru is expected to give a larger N_n in $^{96}\text{Zr}+^{96}\text{Zr}$ collisions than in $^{96}\text{Ru}+^{96}\text{Ru}$ collisions. The free spectator neutrons can be produced either directly or from the deexcitation of charged nucleon clusters. Despite being measured routinely in heavy-ion experiments, the distribution of N_n is mostly used as centrality estimator based on its anticorrelation with the multiplicity N_{ch} of charged particles produced from the QGP matter [37, 38]. Our study is the first to use the N_n to probe the collective structure of colliding nuclei.

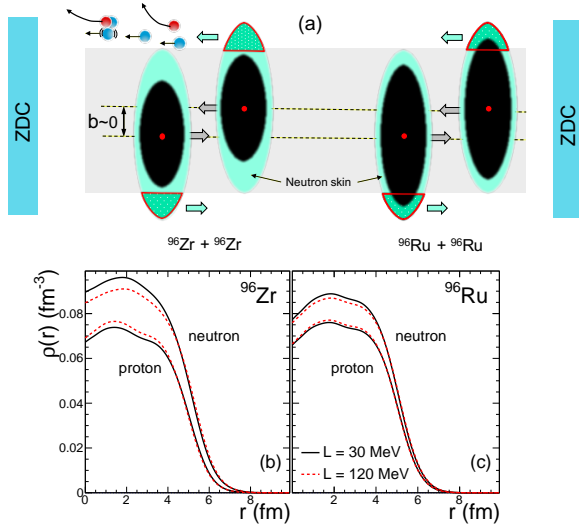


FIG. 1. (top) Side view of central collisions of ^{96}Zr with a larger neutron skin and ^{96}Ru with a smaller neutron skin. The directly-produced spectator neutrons and those from the deexcitation of charged clusters go to the ZDC down the beam-line. The free protons and remaining charged clusters are bent away by beam optics. (bottom) Density profiles of neutrons and protons for ^{96}Zr and ^{96}Ru from spherical SHF calculations using different slope parameter L of symmetry energy.

Method. We generate the spatial distributions of neutrons and protons in the initial ^{96}Zr and ^{96}Ru using the standard Skyrme-Hartree-Fock (SHF) model [39], where the 10 parameters in the Skyrme interaction can be expressed analytically in terms of 10 macroscopic quantities including L . The model allows us to vary L while keeping the other parameters fixed at their empirical values [39] that give a reasonable description of global nuclear structure data. Based on the Skyrme interaction, the energy-density functional can then be obtained using the Hartree-Fock method, and the single-particle Hamil-

tonian is obtained using the variational principle. Solving the Schrödinger equation gives the wave functions of constituent neutrons and protons and thus their density distributions. The effects of quadrupole deformation β_2 are included in the SHF calculation using the cylindrical transformed deformed harmonic oscillator basis [40]. An analysis of the ratio of v_2 and v_3 in the isobar collisions favors $\beta_2 = 0.16$ for ^{96}Ru and $\beta_2 = 0.06$ and $\beta_3 = 0.20$ for ^{96}Zr [31]. Since incorporating the octupole deformation β_3 is much involved, we choose $\beta_{2\text{Zr}} = 0.23$ to compensate the influence of the octupole deformation in ^{96}Zr . We will compare results from spherical and deformed density distributions, and will show later that the results are relatively insensitive to β_2 . The bottom panels of Fig. 1 show the density profiles of ^{96}Zr and ^{96}Ru from spherical SHF calculations. A larger slope parameter $L = 120$ MeV leads to a larger Δr_{np} than $L = 30$ MeV, which is more apparent for the more neutron-rich ^{96}Zr . From the deformed SHF calculation, qualitatively similar effects are observed, while the Δr_{np} can be varied within 10% with different β_2 for the same L , and the β_2 for the distribution of neutrons can be larger than that of protons within about 10%.

The $^{96}\text{Zr}+^{96}\text{Zr}$ and $^{96}\text{Ru}+^{96}\text{Ru}$ collisions are simulated using a Monte-Carlo Glauber model. In each collision event, the colliding nuclei are placed at a random impact parameter and their orientations are uniformly randomized. The coordinates of neutrons and protons are sampled according to the density distributions obtained from the SHF calculation, while their momenta are sampled in the isospin-dependent Fermi sphere according to the local densities of neutrons and protons. The nucleon-nucleon inelastic cross section are chosen to be 42 mb at $\sqrt{s_{NN}} = 200$ GeV. From this, the participant nucleons and spectator nucleons are identified. The quantities associated with participant matter, such as the number of participating nucleons N_{part} and nucleon-nucleon collisions N_{coll} , are calculated for each event. The distribution of these quantities are then used in a fit to the measured distribution of charged-particle multiplicity N_{ch} according to the experimental procedure [30]. The quantities associated with spectator matter, in particular the N_n to be determined below, can then be correlated with N_{ch} , similar to that from the experimental analysis.

The spectator matter are further grouped into charged clusters and free nucleons. Nucleons close in phase space, i.e., with the distance $\Delta r < \Delta r_{\text{max}} = 3$ fm and relative momentum $\Delta p < \Delta p_{\text{max}} = 300$ MeV/c, are assigned to the same cluster [41]. Here Δr_{max} and Δp_{max} represent the scale of maximum distance and relative momentum between neighboring nucleons in the clusters, respectively.

The deexcitation of heavy clusters with $A \geq 4$ are handled by the GEMINI model [42, 43], which requires as inputs the angular momentum and the excitation energy of the cluster. The angular momentum of the cluster is calculated by summing those from all nucleons with respect to their center of mass (C.M.), while the energy of the cluster is calculated from a simplified SHF energy-

density functional [39], with the neutron and proton phase-space information obtained from averaging over parallel events [44, 45] for the same impact parameter and collision orientation. This method can be justified by calculating the binding energy per nucleon based on the ^{96}Zr and ^{96}Ru density distributions as in the bottom panels of Fig. 1, and the results are similar to those obtained from the SHF calculation within ± 1 MeV. The excitation energy is then calculated by subtracting from the calculated cluster energy the ground-state energy of known nuclei taken from Ref. [46]. For clusters with compositions absent in Ref. [46], an improved liquid-drop model [47] is employed to calculate their ground-state energies.

For spectator nucleons that do not form heavy clusters ($A \geq 4$), they still have chances to coalesce into light clusters with $A \leq 3$, i.e., deuterons, tritons, and ^3He , and the formation probabilities are calculated according to the following Wigner functions [48, 49] in their C.M. frame, i.e.,

$$f_d = 8g_d \exp\left(-\frac{\rho^2}{\sigma_d^2} - p_\rho^2 \sigma_d^2\right), \quad (1)$$

$$f_{t/^3\text{He}} = 8^2 g_{t/^3\text{He}} \exp\left[-\left(\frac{\rho^2 + \lambda^2}{\sigma_{t/^3\text{He}}^2}\right) - (p_\rho^2 + p_\lambda^2) \sigma_{t/^3\text{He}}^2\right] \quad (2)$$

with $\vec{\rho} = (\vec{r}_1 - \vec{r}_2)/\sqrt{2}$, $\vec{p}_\rho = (\vec{p}_1 - \vec{p}_2)/\sqrt{2}$, $\vec{\lambda} = (\vec{r}_1 + \vec{r}_2 - 2\vec{r}_3)/\sqrt{6}$, and $\vec{p}_\lambda = (\vec{p}_1 + \vec{p}_2 - 2\vec{p}_3)/\sqrt{6}$ being the relative coordinates and momenta. $g_d = 3/4$ and $g_{t/^3\text{He}} = 1/4$ are the statistical factor for spin 1/2 proton and neutron to form a spin 1 deuteron (spin 1/2 triton/ ^3He), and the width of the Wigner function is chosen to be $\sigma_d = 2.26$ fm, $\sigma_t = 1.59$ fm, and $\sigma_{^3\text{He}} = 1.76$ fm that reproduce the radius of deuterons, tritons, and ^3He [50], respectively. All possible combinations of neutrons and protons are considered in forming light clusters, and this approach has been shown to describe reasonably the production of light clusters in both low- [48] and high-energy [51] heavy-ion collisions. The total free spectator neutrons are composed of the residue neutrons that have not coalesced into light clusters and those from the deexcitation of heavy clusters.

Validation with experimental data. To validate the method and the values of Δr_{max} and Δp_{max} described above, we performed an analysis for Au+Au collisions at $\sqrt{s_{\text{NN}}} = 130$ GeV, for which the experimental data on N_n as a function of N_{ch} exists [52]. The quadrupole deformation is chosen to be $\beta_{2\text{Au}} = -0.15$ [53, 54] and the nucleon-nucleon cross section is taken to be 40 mb. The values of N_n as a function of N_{ch} from our calculation are compared with experimental data in Fig. 2, and here our main focus is on UCC region ($N_{\text{ch}} > 700$), where the results are not affected by uncertainties of cluster deexcitations and other physics processes. A smaller Δr_{max} would imply that nucleons in the nuclear surface, which consists of mostly neutrons, can only combine with close-by nucleons to form clusters, thus there will be more residue free neutrons, compared to the case with a larger

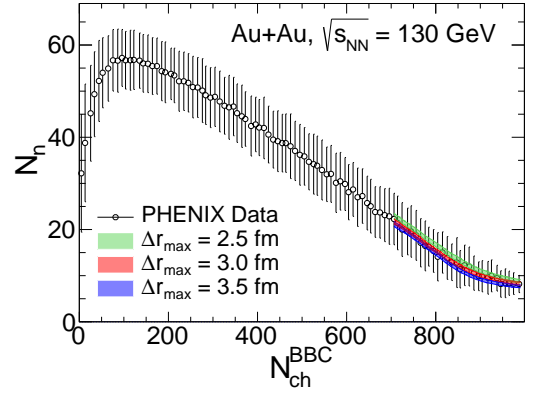


FIG. 2. Comparison of free spectator neutron numbers for three values of Δr_{max} with the RHIC data [52] in Au+Au collisions at $\sqrt{s_{\text{NN}}} = 130$ GeV, at large charged particle multiplicities $N_{\text{ch}}^{\text{BBC}}$ measured by the BBC detector at $3.0 < |\eta| < 3.9$. The error bars on the data represent the RMS width of the correlation. The band for each Δr_{max} indicates the range covered by $L = 30$ to 120 MeV.

Δr_{max} . We see that the value of $\Delta r_{\text{max}} = 3$ fm achieves the best description of the experimental data [52]. We checked that the results are not sensitive to the value of Δp_{max} within its reasonable range.

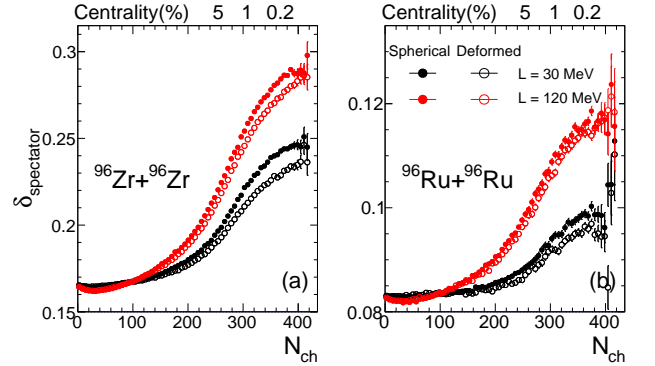


FIG. 3. Isospin asymmetries of spectator matter in $^{96}\text{Zr}+^{96}\text{Zr}$ (a) and $^{96}\text{Ru}+^{96}\text{Ru}$ (b) collision systems with density distributions from spherical or deformed SHF calculations using a smaller or larger L .

Predictions for the isobar systems. Figure 3 displays the overall isospin asymmetry $\delta_{\text{spectator}}$ of the spectator matter as a function of N_{ch} . Due to the presence of neutron skin (see Fig. 1), the spectator matter becomes more neutron rich in more central collisions. Most of the increase, by about 50%, happens over the 0–5% centrality range ($N_{\text{ch}} = 250\text{--}400$), implying that the $\delta_{\text{spectator}}$ in the UCC region is most sensitive to the neutron skin. Furthermore, the more neutron-rich $^{96}\text{Zr}+^{96}\text{Zr}$ system has an overall larger $\delta_{\text{spectator}}$ value than the $^{96}\text{Ru}+^{96}\text{Ru}$ system. Most importantly, for a larger L value and therefore a larger neutron skin, the $\delta_{\text{spectator}}$ in central collisions is greatly enhanced. Inclusion of nuclear deformation

reduces slightly the $\delta_{\text{spectator}}$, since the nuclear deformation, combined with random collision orientation, smears the radial distribution of the spectator protons and neutrons, while such effect is subdominant compared to the influence of L .

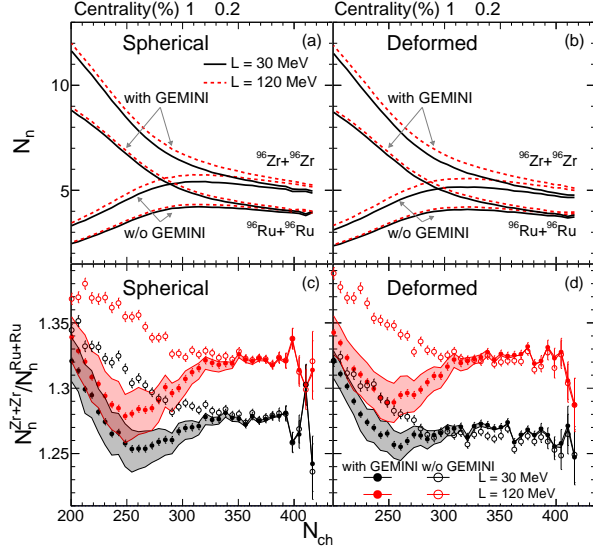


FIG. 4. Number of free spectator neutrons in $^{96}\text{Zr}+^{96}\text{Zr}$ and $^{96}\text{Ru}+^{96}\text{Ru}$ collision systems (upper) as well as their ratios (lower) with density distributions from spherical (left) or deformed (right) SHF calculations using a smaller or larger L .

Figure 4 (a) shows the number of free neutrons N_n with and without considering the deexcitations of heavy clusters in spectator matter via the GEMINI model in the isobar systems. The cluster deexcitations contribute significantly to N_n but are less important in the UCC region of $N_{\text{ch}} > 340$ or centrality range 0 – 0.2%, where N_n with and without deexcitations agree with each other, showing that the deexcitation of heavy clusters is no longer the main contribution to N_n there. On the other hand, we note that among spectator nucleons that do not form heavy clusters, about 0.8 – 1.4 neutrons, dependent on N_{ch} , may coalesce into light clusters. The larger Δr_{np} and thus $\delta_{\text{spectator}}$ associated with $L = 120$ MeV leads to systematically a larger N_n , compared with $L = 30$ MeV. The N_n in a single collision system is susceptible to theoretical and experimental uncertainties, such as clusterization algorithm, excitation energy, or detector efficiency, etc. In contrast, the ratio of N_n in ultracentral $^{96}\text{Zr}+^{96}\text{Zr}$ to $^{96}\text{Ru}+^{96}\text{Ru}$ collisions, as shown in the lower panels of Fig. 4, is a more robust probe of the Δr_{np} in the colliding nuclei free from the uncertainties mentioned above. We predicts a ratio of N_n in the UCC region at around 1.27 for $L = 30$ MeV and 1.32 for $L = 120$ MeV, respectively. The shaded bands in the ratio represent uncertainties from the calculation of the excitation energy (± 1 MeV)

of clusters: a higher excitation energy generally leads to more free nucleons. The ratio in the UCC region of $N_{\text{ch}} > 340$ is clearly insensitive to this uncertainty.

The right panels of Fig. 4 show corresponding results including effects of nuclear deformation. In the UCC region of $N_{\text{ch}} > 340$, the values of N_n are found to decrease by up to 5% compared to the spherical case. However, the ratio of N_n only changes by less than 0.01 when nuclear deformation is enabled, which is much smaller compared to the difference between $L = 30$ and 120 MeV, implying that the potential change to the N_n -ratio associated with uncertainties in the β_2 and β_3 is a subleading effect.

Summary and outlook. We propose that the yield ratio of free spectator neutrons produced in ultracentral relativistic isobaric collisions, which does not suffer from the complex dynamics for observables at midrapidities, is a robust probe of the neutron-skin thickness Δr_{np} of colliding nuclei and the slope parameter L of symmetry energy. We illustrate this idea using a Glauber model for $^{96}\text{Zr}+^{96}\text{Zr}$ and $^{96}\text{Ru}+^{96}\text{Ru}$ collisions, where proton and neutron distributions in ^{96}Zr and ^{96}Ru are provided by the Skyrme-Hartree-Fock calculation, and free spectator neutrons are produced either from the deexcitation of heavy clusters in spectator matter or direct ones that have not coalesced into light clusters. The coalescence parameters for the formation of heavy clusters are tuned to describe measured correlation between the multiplicity of free neutrons N_n and the charged-particle multiplicity near mid-rapidity region in Au+Au collisions. The values of N_n are predicted to be larger in $^{96}\text{Zr}+^{96}\text{Zr}$ than in $^{96}\text{Ru}+^{96}\text{Ru}$ collisions due to larger Δr_{np} in ^{96}Zr than in ^{96}Ru , and the difference between the two system is even larger when a larger L value is used. We found that the ratio of N_n in ultracentral collisions are free from the uncertainties of cluster deexcitations and is relatively insensitive to the nuclear deformation. This ratio is also expected to largely cancel experimental errors, therefore making it an ideal probe of the Δr_{np} of colliding nuclei.

The present study can be generalized to any two colliding systems with similar mass number but different isospin asymmetries such as those along an isotopic chain, for which the sensitivity of the N_n -ratio to Δr_{np} and L is expected to increase with increasing difference in their isospin asymmetries. For a single colliding system, such as Au+Au or Pb+Pb, we found that the yield ratio of free spectator neutrons over free spectator protons is also an excellent probe of Δr_{np} and L . The free spectator protons can be measured by instrumenting the forward region with dedicated detectors, see, e.g., Ref. [55]. Such study is in progress.

JX and JZ are supported by the National Natural Science Foundation of China under Grant No. 11922514. JJ and CZ are supported by the US Department of Energy under Contract No. DEFG0287ER40331. GXP and LL are supported by the National Natural Science Foundation of China under Grant Nos. 11875052, 11575190, and 11135011.

-
- [1] B. Alex Brown, “Neutron radii in nuclei and the neutron equation of state,” *Phys. Rev. Lett.* **85**, 5296–5299 (2000).
- [2] S. Typel and B. Alex Brown, “Neutron radii and the neutron equation of state in relativistic models,” *Phys. Rev. C* **64**, 027302 (2001).
- [3] M. Thiel, C. Sienti, J. Piekarewicz, C. J. Horowitz, and M. Vanderhaeghen, “Neutron skins of atomic nuclei: per aspera ad astra,” *J. Phys. G* **46**, 093003 (2019), [arXiv:1904.12269 \[nucl-ex\]](#).
- [4] C. J. Horowitz and J. Piekarewicz, “Neutron star structure and the neutron radius of Pb-208,” *Phys. Rev. Lett.* **86**, 5647 (2001), [arXiv:astro-ph/0010227](#).
- [5] R. J. Furnstahl, “Neutron radii in mean field models,” *Nucl. Phys. A* **706**, 85–110 (2002), [arXiv:nucl-th/0112085](#).
- [6] B. G. Todd-Rutel and J. Piekarewicz, “Neutron-Rich Nuclei and Neutron Stars: A New Accurately Calibrated Interaction for the Study of Neutron-Rich Matter,” *Phys. Rev. Lett.* **95**, 122501 (2005), [arXiv:nucl-th/0504034](#).
- [7] M. Centelles, X. Roca-Maza, X. Vinas, and M. Warda, “Nuclear symmetry energy probed by neutron skin thickness of nuclei,” *Phys. Rev. Lett.* **102**, 122502 (2009), [arXiv:0806.2886 \[nucl-th\]](#).
- [8] Zhen Zhang and Lie-Wen Chen, “Constraining the symmetry energy at subsaturation densities using isotope binding energy difference and neutron skin thickness,” *Phys. Lett. B* **726**, 234–238 (2013), [arXiv:1302.5327 \[nucl-th\]](#).
- [9] Jun Xu, Wen-Jie Xie, and Bao-An Li, “Bayesian inference of nuclear symmetry energy from measured and imagined neutron skin thickness in $^{116,118,120,122,124,130,132}\text{Sn}$, ^{208}Pb , and ^{48}Ca ,” *Phys. Rev. C* **102**, 044316 (2020), [arXiv:2007.07669 \[nucl-th\]](#).
- [10] Andrew W. Steiner, Madappa Prakash, James M. Lattimer, and Paul J. Ellis, “Isospin asymmetry in nuclei and neutron stars,” *Phys. Rept.* **411**, 325–375 (2005), [arXiv:nucl-th/0410066](#).
- [11] James M. Lattimer and Madappa Prakash, “Neutron Star Observations: Prognosis for Equation of State Constraints,” *Phys. Rept.* **442**, 109–165 (2007), [arXiv:astro-ph/0612440](#).
- [12] Bao-An Li, Lie-Wen Chen, and Che Ming Ko, “Recent Progress and New Challenges in Isospin Physics with Heavy-Ion Reactions,” *Phys. Rept.* **464**, 113–281 (2008), [arXiv:0804.3580 \[nucl-th\]](#).
- [13] A. Trzcinska, J. Jastrzebski, P. Lubinski, F. J. Hartmann, R. Schmidt, T. von Egidy, and B. Klos, “Neutron density distributions deduced from anti-protonic atoms,” *Phys. Rev. Lett.* **87**, 082501 (2001).
- [14] B. Klos *et al.*, “Neutron density distributions from antiprotonic Pb-208 and Bi-209 atoms,” *Phys. Rev. C* **76**, 014311 (2007), [arXiv:nucl-ex/0702016](#).
- [15] B. Alex Brown, G. Shen, G. C. Hillhouse, Jie Meng, and A. Trzcinska, “Neutron skin deduced from antiprotonic atom data,” *Phys. Rev. C* **76**, 034305 (2007).
- [16] S. Terashima *et al.*, “Proton elastic scattering from tin isotopes at 295-MeV and systematic change of neutron density distributions,” *Phys. Rev. C* **77**, 024317 (2008), [arXiv:0801.3082 \[nucl-ex\]](#).
- [17] J. Zenihiro *et al.*, “Neutron density distributions of Pb-204, Pb-206, Pb-208 deduced via proton elastic scattering at $E_p=295$ MeV,” *Phys. Rev. C* **82**, 044611 (2010).
- [18] E. Friedman, “Neutron skins of ^{208}Pb and ^{48}Ca from pionic probes,” *Nucl. Phys. A* **896**, 46–52 (2012), [arXiv:1209.6168 \[nucl-ex\]](#).
- [19] C. M. Tarbert *et al.*, “Neutron skin of ^{208}Pb from Coherent Pion Photoproduction,” *Phys. Rev. Lett.* **112**, 242502 (2014), [arXiv:1311.0168 \[nucl-ex\]](#).
- [20] S. Abrahamyan *et al.*, “Measurement of the Neutron Radius of ^{208}Pb Through Parity-Violation in Electron Scattering,” *Phys. Rev. Lett.* **108**, 112502 (2012), [arXiv:1201.2568 \[nucl-ex\]](#).
- [21] D. Adhikari *et al.* (PREX), “Accurate Determination of the Neutron Skin Thickness of ^{208}Pb through Parity-Violation in Electron Scattering,” *Phys. Rev. Lett.* **126**, 172502 (2021), [arXiv:2102.10767 \[nucl-ex\]](#).
- [22] Brendan T. Reed, F. J. Fattoyev, C. J. Horowitz, and J. Piekarewicz, “Implications of PREX-2 on the Equation of State of Neutron-Rich Matter,” *Phys. Rev. Lett.* **126**, 172503 (2021), [arXiv:2101.03193 \[nucl-th\]](#).
- [23] J. Piekarewicz, “Implications of PREX-2 on the electric dipole polarizability of neutron-rich nuclei,” *Phys. Rev. C* **104**, 024329 (2021), [arXiv:2105.13452 \[nucl-th\]](#).
- [24] Mattia Atzori Corona, Matteo Cadeddu, Nicola Cargioli, Paolo Finelli, and Matteo Vorabbi, “Incorporating the weak mixing angle dependence to reconcile the neutron skin measurement on ^{208}Pb by PREX-II,” (2021), [arXiv:2112.09717 \[hep-ph\]](#).
- [25] Peter Filip, Richard Lednicky, Hiroshi Masui, and Nu Xu, “Initial eccentricity in deformed Au-197 + Au-197 and U-238 + U-238 collisions at $\sqrt{s_{NN}}=200$ GeV at the BNL Relativistic Heavy Ion Collider,” *Phys. Rev. C* **80**, 054903 (2009).
- [26] Q. Y. Shou, Y. G. Ma, P. Sorensen, A. H. Tang, F. Videbæk, and H. Wang, “Parameterization of Deformed Nuclei for Glauber Modeling in Relativistic Heavy Ion Collisions,” *Phys. Lett. B* **749**, 215–220 (2015), [arXiv:1409.8375 \[nucl-th\]](#).
- [27] Giuliano Giacalone, “Observing the deformation of nuclei with relativistic nuclear collisions,” *Phys. Rev. Lett.* **124**, 202301 (2020), [arXiv:1910.04673 \[nucl-th\]](#).
- [28] Hanlin Li, Hao-jie Xu, Ying Zhou, Xiaobao Wang, Jie Zhao, Lie-Wen Chen, and Fuqiang Wang, “Probing the neutron skin with ultrarelativistic isobaric collisions,” *Phys. Rev. Lett.* **125**, 222301 (2020), [arXiv:1910.06170 \[nucl-th\]](#).
- [29] Jiangyong Jia, “Shape of atomic nuclei in heavy ion collisions,” *Phys. Rev. C* **105**, 014905 (2022), [arXiv:2106.08768 \[nucl-th\]](#).
- [30] Mohamed Abdallah *et al.* (STAR), “Search for the chiral magnetic effect with isobar collisions at $\sqrt{s_{NN}}=200$ GeV by the STAR Collaboration at the BNL Relativistic Heavy Ion Collider,” *Phys. Rev. C* **105**, 014901 (2022), [arXiv:2109.00131 \[nucl-ex\]](#).
- [31] Chunjian Zhang and Jiangyong Jia, “Evidence of Quadrupole and Octupole Deformations in $\text{Zr}96+\text{Zr}96$ and $\text{Ru}96+\text{Ru}96$ Collisions at Ultrarelativistic Energies,” *Phys. Rev. Lett.* **128**, 022301 (2022), [arXiv:2109.01631 \[nucl-th\]](#).
- [32] Jiangyong Jia and Chun-Jian Zhang, “Scaling approach to nuclear structure in high-energy heavy-ion collisions,”

- (2021), [arXiv:2111.15559 \[nucl-th\]](#).
- [33] Hao-jie Xu, Wenbin Zhao, Hanlin Li, Ying Zhou, Lie-Wen Chen, and Fuqiang Wang, “Probing nuclear structure with mean transverse momentum in relativistic isobar collisions,” (2021), [arXiv:2111.14812 \[nucl-th\]](#).
 - [34] Jiangyong Jia, “Probing triaxial deformation of atomic nuclei in high-energy heavy ion collisions,” (2021), [arXiv:2109.00604 \[nucl-th\]](#).
 - [35] Benjamin Bally, Michael Bender, Giuliano Giacalone, and Vittorio Somà, “Evidence of the Triaxial Structure of Xe129 at the Large Hadron Collider,” *Phys. Rev. Lett.* **128**, 082301 (2022), [arXiv:2108.09578 \[nucl-th\]](#).
 - [36] Jiangyong Jia, Shengli Huang, and Chunjian Zhang, “Probing nuclear quadrupole deformation from correlation of elliptic flow and transverse momentum in heavy ion collisions,” *Phys. Rev. C* **105**, 014906 (2022), [arXiv:2105.05713 \[nucl-th\]](#).
 - [37] K. Adcox *et al.* (PHENIX), “Centrality dependence of charged particle multiplicity in Au - Au collisions at $S(NN)^{1/2} = 130$ -GeV,” *Phys. Rev. Lett.* **86**, 3500–3505 (2001), [arXiv:nucl-ex/0012008](#).
 - [38] Betty Abelev *et al.* (ALICE), “Centrality determination of Pb-Pb collisions at $\sqrt{s_{NN}} = 2.76$ TeV with ALICE,” *Phys. Rev. C* **88**, 044909 (2013), [arXiv:1301.4361 \[nucl-ex\]](#).
 - [39] Lie-Wen Chen, Che Ming Ko, Bao-An Li, and Jun Xu, “Density slope of the nuclear symmetry energy from the neutron skin thickness of heavy nuclei,” *Phys. Rev. C* **82**, 024321 (2010), [arXiv:1004.4672 \[nucl-th\]](#).
 - [40] M. V. Stoitsov, N. Schunck, M. Kortelainen, N. Michel, H. Nam, E. Olsen, J. Sarich, and S. Wild, “Axially deformed solution of the Skyrme-Hartree-Fock-Bogolyubov equations using the transformed harmonic oscillator basis (II) HFBTHO v2.00c: a new version of the program,” *Comput. Phys. Commun.* **184**, 1592–1604 (2013), [arXiv:1210.1825 \[nucl-th\]](#).
 - [41] Bao-An Li, C. M. Ko, and Zhong-zhou Ren, “Equation of state of asymmetric nuclear matter and collisions of neutron rich nuclei,” *Phys. Rev. Lett.* **78**, 1644 (1997), [arXiv:nucl-th/9701048](#).
 - [42] R. J. Charity *et al.*, “Systematics of complex fragment emission in niobium-induced reactions,” *Nucl. Phys. A* **483**, 371–405 (1988).
 - [43] R. J. Charity, “A Systematic description of evaporation spectra for light and heavy compound nuclei,” *Phys. Rev. C* **82**, 014610 (2010), [arXiv:1006.5018 \[nucl-th\]](#).
 - [44] Cheuk-Yin Wong, “Dynamics of nuclear fluid. VIII. Time-dependent Hartree-Fock approximation from a classical point of view,” *Phys. Rev. C* **25**, 1460–1475 (1982).
 - [45] G. F. Bertsch and S. Das Gupta, “A Guide to microscopic models for intermediate-energy heavy ion collisions,” *Phys. Rept.* **160**, 189–233 (1988).
 - [46] Meng Wang, W. J. Huang, F. G. Kondev, G. Audi, and S. Naimi, “The AME 2020 atomic mass evaluation (II). Tables, graphs and references,” *Chin. Phys. C* **45**, 030003 (2021).
 - [47] Ning Wang, Min Liu, Xizhen Wu, and Jie Meng, “Surface diffuseness correction in global mass formula,” *Phys. Lett. B* **734**, 215–219 (2014), [arXiv:1405.2616 \[nucl-th\]](#).
 - [48] Lie-Wen Chen, C. M. Ko, and Bao-An Li, “Light cluster production in intermediate-energy heavy ion collisions induced by neutron rich nuclei,” *Nucl. Phys. A* **729**, 809–834 (2003), [arXiv:nucl-th/0306032](#).
 - [49] Kai-Jia Sun and Lie-Wen Chen, “Analytical coalescence formula for particle production in relativistic heavy-ion collisions,” *Phys. Rev. C* **95**, 044905 (2017), [arXiv:1701.01935 \[nucl-th\]](#).
 - [50] G. Ropke, “Light nuclei quasiparticle energy shift in hot and dense nuclear matter,” *Phys. Rev. C* **79**, 014002 (2009), [arXiv:0810.4645 \[nucl-th\]](#).
 - [51] Wenbin Zhao, Chun Shen, Che Ming Ko, Quansheng Liu, and Huichao Song, “Beam-energy dependence of the production of light nuclei in Au + Au collisions,” *Phys. Rev. C* **102**, 044912 (2020), [arXiv:2009.06959 \[nucl-th\]](#).
 - [52] Mickey Chu, “PHENIX focus: Zero Degree Calorimeter,” https://zenodo.org/record/4008646/files/focus_zdc.pdf (2002).
 - [53] Giuliano Giacalone, Jiangyong Jia, and Chunjian Zhang, “Impact of Nuclear Deformation on Relativistic Heavy-Ion Collisions: Assessing Consistency in Nuclear Physics across Energy Scales,” *Phys. Rev. Lett.* **127**, 242301 (2021), [arXiv:2105.01638 \[nucl-th\]](#).
 - [54] P. Möller, A. J. Sierk, T. Ichikawa, and H. Sagawa, “Nuclear ground-state masses and deformations: FRDM(2012),” *Atom. Data Nucl. Data Tabl.* **109-110**, 1–204 (2016), [arXiv:1508.06294 \[nucl-th\]](#).
 - [55] Sourav Tarafdar, Zvi Citron, and Alexander Milov, “A Centrality Detector Concept,” *Nucl. Instrum. Meth. A* **768**, 170–178 (2014), [arXiv:1405.4555 \[nucl-ex\]](#).